DOI: 10.1002/chem.200600037

Effect of Polarity and Structural Design on Molecular Photorefractive Properties of Heteroaromatic-Based Push–Pull Dyes

Graziano Archetti,[a, b] Alessandro Abbotto,*[a] and Rüdiger Wortmann*[b, c]

Abstract: A combined experimental (optical and electro-optical absorption measurements) and computational (ab initio RHF and DFT) approach has been used to investigate the molecular low- and high-T_g photorefractive (PR) performances of neutral and zwitterionic heteroaromatic dipolar chromophores in terms of structural and solvent-polarity effects. We have found that the nature of the building units (donor, acceptor, and spacer) and the polarity of the surrounding medium strongly affect all the relevant ground-state and nonlinear optical properties involved in the PR activity, that is, the dipole moment, the polarizability anisotropy, and first hyperpolarizability of the electronic ground-state. The variation of these properties is in turn transferred to molecular low- and high-T_g PR figures of merit. It is shown that PR molecular performance not only relies on a proper choice of structural components but varies by orders of magnitude as a function of the medium polarity, and this suggests that a combination of molecular design and host-matrix engineering is required for optimized performances of PR materials.

Keywords: ab initio calculations · donor–acceptor systems · dyes/pigments · nonlinear optics · solvent effects

Introduction

The photorefractive (PR) effect refers to spatial modulation of the refractive index of a material under nonuniform illumination via space–charge field formation and electro-optical nonlinearity. It arises in materials combining photosensitivity and conductivity when charge carriers, photogenerated by a spatially modulated light intensity, separate and become trapped to produce a nonuniform space–charge distribution which leads to the formation of an internal modulated space–charge field (E_{SC}). The interaction of E_{SC} with the materials modulates the refractive index to create a phase grating, or hologram, which can diffract a light beam.[1] Photorefractivity in organic amorphous materials is achieved by combining appropriate functional molecules or moieties to impart photosensitivity, conductivity, and electro-optical (EO) response.[2] This effect was first reported in polymeric materials in 1991.[3] Typical EO chromophores are push–pull systems consisting of a π-electron bridge end-capped by π-electron-donor (D) and π-electron-acceptor (A) groups (Scheme 1). In the case of an amorphous material, we can distinguish two cases: its glass-transition temperature T_g is either higher or is approximately equal to room temperature (working temperature). In the former type (high-T_g materials) phase-grating formation can be attributed to a linear electro-optical Pockels effect ($\chi^{(2)}$).[4] Since the isotropic material would yield no electro-optical effect, the PR effect arises from materials which have been previously poled by an external electric field. In the second case (low-T_g materials) a second-order electro-optical Kerr effect ($\chi^{(3)}$) is present in addition to the Pockels effect.[5] In low-T_g materials reorientation of the dipolar chromophores plays an im-

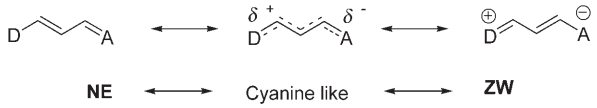

Scheme 1. Resonance limit structures (**NE** = neutral; **ZW** = zwitterionic) of push–pull molecules (D = electron-donor group, A = electron-acceptor group).

[a] Dr. G. Archetti, Prof. Dr. A. Abbotto
Department of Materials Science and INSTM
University of Milano-Bicocca
Via Cozzi 53, 20125 Milano (Italy)
Fax: (+39) 02-6448-5400
E-mail: alessandro.abbotto@unimib.it

[b] Dr. G. Archetti, Prof. Dr. R. Wortmann
Department of Physical Chemistry
Technical University of Kaiserslautern
Erwin-Schroedinger-Strasse, 67663, Kaiserslautern (Germany)

[c] Prof. Dr. R. Wortmann
Deceased, March 13, 2005

Supporting information for this article is available on the WWW under http://www.chemeurj.org/ or from the author.

portant role (orientational enhancement effect).[6] On the basis of the microscopic interpretation of these two effects,[5,7] Equations (1) and (2) have been proposed as figures-of-merit to give a useful tool for predicting the PR performances of EO chromophores

$$F_{\omega}^{L} = \frac{1}{M}\left[9\mu_g\beta(-\omega;\omega,0) + \frac{2\mu_g^2\delta\alpha(-\omega;\omega)}{k_B T}\right] \quad (1)$$

$$F_{\omega}^{H} = \frac{\mu_g\beta(-\omega;\omega,0)}{M} \quad (2)$$

where k_B is the Boltzmann constant, T the working temperature, F_{ω}^{L} and F_{ω}^{H} are the figures of merit for low-T_g ($T \approx T_g$) and high-T_g ($T < T_g$) PR materials, respectively, M is the molar mass of the chromophores, μ_g the ground-state dipole moment (the z axis is chosen to be parallel to μ_g), $\beta(-\omega;\omega,0)$ the second-order polarizability, and $\delta\alpha(-\omega;\omega)$ the anisotropy of the optical polarizability, which can be written in the form of Equation (3) , where α_{ii} ($i = x, y, z$) are the diagonal elements of the polarizability tensor.

$$\delta\alpha = \alpha_{zz} - 1/2(\alpha_{yy} + \alpha_{xx}) \quad (3)$$

The molecular properties involved in Equations (1) and (2) depend on the ground-state electronic distribution of the EO chromophores. The ground state of a push–pull system, as shown in Scheme 1, can be represented in terms of zwitterionic (**ZW**) and neutral (**NE**) limiting structures. The relative weight of the two limit forms depends on the electron affinities of A and D, on the type of π-conjugated bridge, and on the polarity ε_r of the surrounding medium.[8,9] In the last decade different parameters have been proposed (c^2, BLA, and MIX)[5,10] to describe the polarization of the ground state and to show the relationship between electronic distribution and ground-state properties. According to a simple two-level model (TLM),[11] $\delta\alpha(-\omega;\omega)$ and $\beta(-\omega;\omega,0)$ vanish at the **ZW** limit ($c^2 = 1$), where μ_g is maximized. In contrast, $\delta\alpha(-\omega;\omega)$ finds its maximum at the so-called cyanine limit ($c^2 = 0.5$), where $\beta(-\omega;\omega,0)$ is again equal to zero.[7]

While several contributions have reported on the relationships between structural parameters and ground-state electronic distribution, leading to design principles for EO chromophores,[1,5,8,12,13] the effect of systematic variation of the surrounding polarity on the PR figures of merit has been scantly investigated, in spite of its important role in affecting the ground-state parameters. In particular, we were attracted by the idea of affecting the PR molecular efficiency through a fine rearrangement of the ground-state electronic distribution on varying the polarity of the surrounding medium.

For our purposes we selected two series of azinium-based derivatives that we have previously investigated for their large tunability of molecular ground-state properties: 1) pyridoneimines **1** and **2** and pyridonemethides **3** and **4**;[14] 2) azinium dicyanomethanido zwitterions **5** and **6**.[9,15,16]

These two classes of push–pull dyes were particularly suitable for the following reasons: 1) they were expected to have different and variable **NE** or **ZW** characters (Scheme 2) and

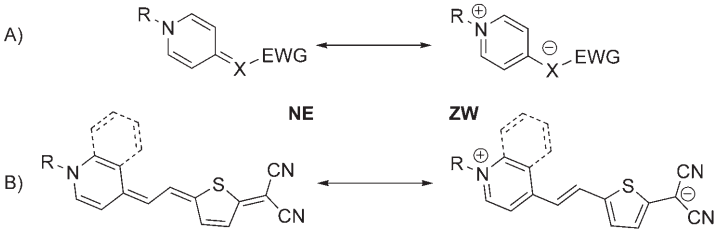

Scheme 2. Neutral (**NE**) and zwitterionic (**ZW**) resonance limit structures of dyes **1**–**4** (A), and **5** and **6** (B).

thus affect the PR figures of merit in a significantly different manner;[17] 2) aromatic and quinoid heterocycles usually impart a larger degree of polarization of the π-conjugated framework than a simple donor–acceptor polyene; 3) molecules with large ground-state dipole moments are highly sensitive to the surrounding medium.[9] These factors, combined with the effect of the surrounding polarity, should lead to a variety of different structural and electronic properties.

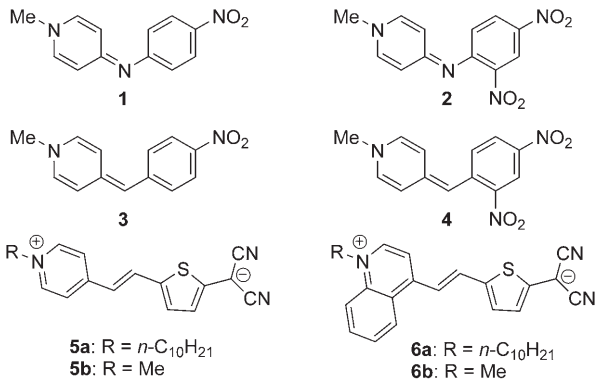

We felt that surrounding-polarity effects could be properly investigated by considering an adequate set of solvents covering a polarity range as large as possible. To this end, we selected the following solvents from low to high dielectric constant: 1,4-dioxane ($\varepsilon_r = 2.2$), $CHCl_3$ ($\varepsilon_r = 4.8$), acetone ($\varepsilon_r = 20.7$), and DMSO ($\varepsilon_r = 46.7$). These solvents are widely used for organic EO chromophores. The electro-optical absorption (EOA) approach[7,18] seemed an appropriate choice to experimentally access all of the molecular parameters appearing in the aforementioned figures of merit. However, the inherent limitations to apolar or low-polarity solvents prompted us to use a judicious combination of experiments (optical and electro-optical absorption spectroscopy) and computations (ab initio quantum chemical calculations) to thoroughly investigate the dependence of the PR performances of chromophores **1**–**6** on structural effects and surrounding polarity.

Results and Discussion

Optical investigation: The optical absorption spectra of push–pull molecules are often characterized by a strong absorption band at low energy corresponding to intramolecular charge transfer (CT) between the donor and the acceptor moieties. According to the TLM and adopting the Taylor convention[19] Equations (4) and (5) can be derived, where $\delta\alpha_0$ and β_0 are the TLM approximations for $\delta\alpha(-0;0)$ and $\beta(-0;0,0)$, respectively, $\Delta\mu$ and μ_{eg} the change of the dipole moment and the electronic transition dipole moment on electronic excitation from the ground to the excited state, and λ_{eg} is the wavelength of the optical excitation associated with the CT transition. All of these properties can be obtained by careful analysis of the CT band.[5a,9] Furthermore, the resonance structures of the chromophores and the maximal hypothetical dipole change $\Delta\mu_{max}$ (defined as the difference in dipole moments of the pure **ZW** and **NE** structures) can be described in terms of the resonance parameter c^2 according to Equations (6) and (7).[7]

$$\delta\alpha_0 = \frac{2\mu_{eg}^2\lambda_{eg}}{hc} \quad (4)$$

$$\beta_0 = \frac{6(\mu_{eg}\lambda_{eg})^2\Delta\mu}{(hc)^2} \quad (5)$$

$$c^2 = \frac{1}{2}[1-\Delta\mu(4\mu_{eg}^2+\Delta\mu^2)^{-1/2}] \quad (6)$$

$$\Delta\mu_{max} = \frac{\Delta\mu}{1-2c^2} \quad (7)$$

Table 1. Solvatochromic data (λ_{eg}/nm) of the CT band for the chromophores **1**–**4**, **5a**, and **6a** in selected solvents.

(ε_r)	1,4-Dioxane (2.2)	$CHCl_3$ (4.8)	Acetone (20.7)	DMSO (46.7)	$\Delta\tilde{\nu}$ [cm^{-1}][a]
1	409	413	432	458	2380
2	423	432	449	467	1730
3	520	539	550	590	1600
4	559	580	579	595	440
5a	709	706	645	621	−1940
6a	762	765	737	718	−860

[a] $\Delta\tilde{\nu}=\tilde{\nu}(CHCl_3)-\tilde{\nu}(DMSO)$: positive $\Delta\tilde{\nu}$ values mean positive solvatochromism.

UV/Vis spectroscopy: All of the chromophores show an intense CT band in the visible region of the spectrum. Tables 1 and 2 (see also Supporting Information) collect UV/Vis data (λ_{eg}, ε; CT band) and the derived electronic properties (μ_{eg}, $\delta\alpha_0$) as a function of ε_r. See Supporting Information for UV/Vis absorption spectra of **1**–**4**, **5a**, and **6a** in solvents of different polarity.

Compounds **1**–**4** show positive solvatochromism. The addition of a second nitro group in the phenyl rings of **2** and **4** leads to a bathochromic shift in comparison to mononitro derivatives **1** and **3**, in accordance with an increase in electron-acceptor strength. The increase in solvent polarity acts to mitigate the difference between *p*-nitrophenyl and 2,4-dinitrophenyl electron affinities. In the comparison between the N-bridged and the corresponding methino derivatives (**1** vs. **3** and **2** vs. **4**) a considerable shift of the CT band to longer wavelength and a hyperchromic effect are observed.

Table 2. Experimental[a] and computed[b] ground-state dipole moment μ_g, polarizability anisotropy $\delta\alpha_0$, and first hyperpolarizability β_0 of compounds **1**–**6** in selected media.[c]

		Gas phase (1.0)			1,4-dioxane (2.2)			$CHCl_3$ (4.8)			Acetone (20.7)			DMSO (46.7)		
(ε_r)		μ_g	$\delta\alpha_0$	β_0	μ_g	$\delta\alpha_0$	β_0	μ_g	$\delta\alpha_0$	β_0	μ_g	$\delta\alpha_0$	β_0	μ_g	$\delta\alpha_0$	β_0
1	exptl				28.6	17	56		19			22			–[d]	
	comp	39.8	24	4	44.9	29	8	49.1	34	14	53.4	39	22	54.4	40	24
		(41.6)	(36)		(47.7)	(44)		(52.9)	(52)		(58.4)	(60)		(59.6)	(62)	
2	exptl				27.6	15	45		–[d]			22			26	
	comp	40.8	20	2	48.7	26	5	55.3	31	9	62.1	37	15	63.6	38	16
		(44.9)	(30)		(53.2)	(39)		(60.3)	(46)		(67.8)	(55)		(69.4)	(57)	
3	exptl				27.2	37	146		–[d]			45			55	
	comp	35.0	32	18	40.3	41	33	44.8	48	52	49.8	57	80	51.0	59	88
		(40.5)	(51)		(48.6)	(67)		(55.8)	(82)		(63.8)	(98)		(65.6)	(101)	
4	exptl				28.2	37	87		–[d]			45			48	
	comp	39.2	30	18	46.1	39	32	52.8	47	48	61.4	58	63	63.7	61	64
		(46.5)	(47)		(57.3)	(62)		(67.2)	(76)		(78.1)	(89)		(80.5)	(91)	
5[e]	exptl[f]				66.7	98	−92		113			93			76	
	comp[g]	61.4	81	25	90.5	124	−45	152.8	87	−310	177.4	65	−131	181.0	63	−113
		(67.8)	(104)		(94.1)	(142)		(125.2)	(166)		(162.4)	(145)		(169.5)	(136)	
6[e]	exptl[f]				56.2	104	66		144			131			118	
	comp[g]	55.4	84	33	80.8	131	46	158.8	93	−339	186.4	70	−120	190.9	68	−98
		(62.7)	(115)		(91.8)	(169)		(131.3)	(202)		(178.7)	(154)		(186.9)	(144)	

[a] From optical and electro-optical absorption measurements. [b] From RHF/6-31G*//RHF/6-31G* and B3LYP/6-31G*//B3LYP/6-31G* (in parentheses) ab initio calculations; **1**–**4**: C_1 symmetry; **5b** and **6b**: C_s symmetry. [c] $\mu_g/10^{-30}$ Cm; $\delta\alpha_0/10^{-40}$ $CV^{-1}m^2$; $\beta_0=\beta_{0,vec}/10^{-50}$ $CV^{-2}m^3$; data were calculated according to the Taylor convention.[9] [d] Experimental data not available. [e] Experimental and computed RHF/6-31G*//RHF/6-31G* μ_g and β_0 values are from ref. [9]. [f] Derivatives **a**. [g] Derivatives **b**.

The induced shift is much larger than that caused by the addition of the second nitro group.

The increased conjugation of the π spacer (CH=CH unit and thiophene ring) and the different strength of the acceptor group (dicyanomethanido moiety) lead to a bathochromic shift of the CT band in **5a** and **6a** with respect to dyes **1**–**4**. We have previously shown[9] that these chromophores have a dual nature in terms of ground-state polarization. An **NE** ground-state character predominates in low-polarity solvents, whereas the **ZW** limiting form better describes the electronic distribution in high-polarity solvents. The effect of the annelation (benzo fusion of the acceptor azinium ring from **5a** to **6a**) shifts the ε_r point where predominant **NE** character switches to predominant **ZW** character (ε_{rL}).

The polarizability anisotropy $\delta\alpha_0$ and the transition dipole moment μ_{eg} significantly depend on ε_r. The trends followed by the two classes of chromophores are opposite. The μ_{eg} value decreases for **5a** and **6a** on increasing the polarity of the solvent, whereas it slightly increases for **1**–**4**. The same trend is observed for the $\delta\alpha_0$ values. A considerable drop in the $\delta\alpha_0$ values of **5a** and **6a** is recorded on going from $CHCl_3$ to more polar solvents.

Electro-optical and nonlinear optical properties: EOA spectroscopy is a powerful experimental technique that can be used for characterizing the CT band of a push–pull molecule.[7,18] In an EOA experiment one measures the effect of an externally applied electric field on the molar decadic absorption coefficient ε. The absorption coefficient in the presence of the field ε^E is a even function of the applied field E and is traditionally approximated to Equation (8).

$$\varepsilon^E(\phi,\tilde{\nu}) = \varepsilon(\tilde{\nu})[1 + L(\phi,\tilde{\nu})E^2 + \ldots] \quad (8)$$

The relative change induced by the field L is a function of the wavenumber $1/\lambda$ and of the angle φ between the plane of polarization of the incident light and the applied electric field. A multilinear regression analysis of the band shape and of the band shift (usually represented in the form $L\varepsilon/\tilde{\nu}$) in terms of the first and second derivatives of the optical absorption spectrum yields a set of regression coefficients D, E, F, G, H, and I from which the ground-state dipole moment μ_g and the dipole difference $\Delta\mu$ can be calculated.[20]

Figure 1 shows EOA spectra recorded in 1,4-dioxane and multilinear fittings for 0 and 90° of polarization of the incident light for azomethine derivative **2** and methine derivative **4**, taken as examples (spectra of corresponding mononitro derivatives are shown in the Supporting Information). Results of the EOA measurements and values of the derived molecular properties of **1**–**4** are listed in

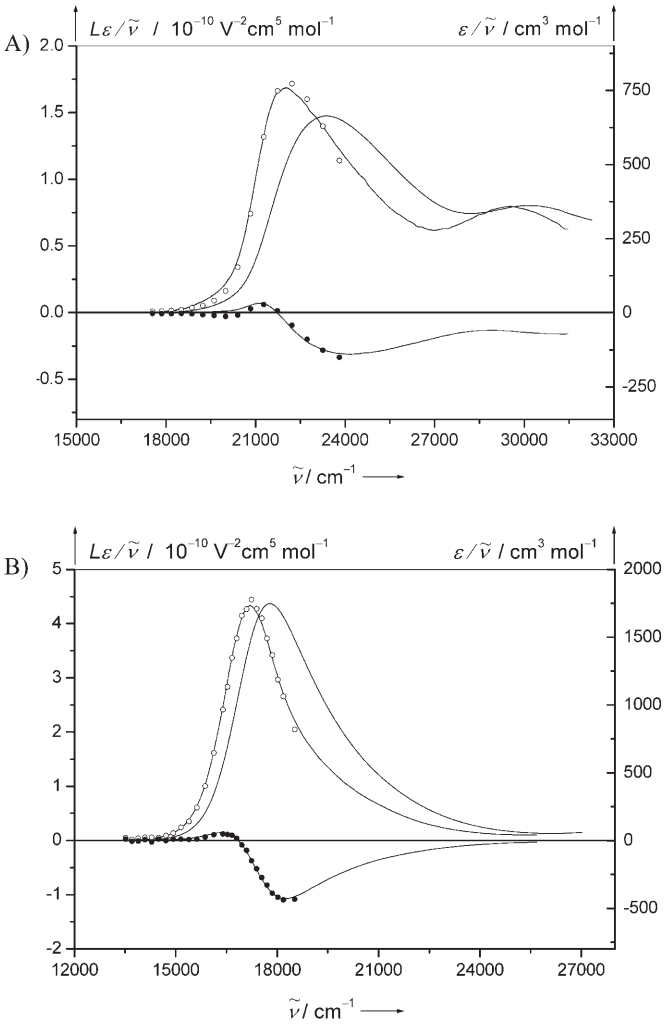

Figure 1. Optical ($\varepsilon/\tilde{\nu}$) and electro-optical absorption spectra ($L\varepsilon/\tilde{\nu}$) of **2** (A) and **4** (B) in 1,4-dioxane, $T = 298$ K. Data points for parallel (○: $\varphi = 0°$) and perpendicular (●: $\varphi = 90°$) polarization of the incident light relative to the applied electric field and multilinear regression curves.

Table 3. Dipole differences were calculated from the average values of the regression coefficients F and G, whereas the ground-state dipole moment was obtained from the difference $E - 6D$.[20] The β_0 values, calculated from data of Table 3 according to Equation (5), are collected in Table 2.

Table 3. Results of EOA measurements in 1,4-dioxane ($T = 298$ K) for dyes **1**–**4**: multilinear fitting coefficients and derived molecular properties.

Parameter	Units	**1**	**2**	**3**	**4**
D	10^{-20} V^{-2} m^2	790 ± 40	1630 ± 180	1080 ± 70	1500 ± 60
E	10^{-20} V^{-2} m^2	27000 ± 210	30480 ± 1090	26660 ± 400	30610 ± 370
F	10^{-40} CV^{-1} m^2	8660 ± 160	7070 ± 980	8320 ± 230	4790 ± 230
G	10^{-40} CV^{-1} m^2	9480 ± 160	8700 ± 980	8020 ± 230	4860 ± 230
μ_g	10^{-30} Cm	28.6 ± 0.2	27.6 ± 1.0	27.2 ± 0.4	28.2 ± 0.3
$\Delta\mu$	10^{-30} Cm	54.1 ± 0.7	46.2 ± 4.2	50.0 ± 1.1	28.0 ± 1.0
$\Delta\mu_{max}$	10^{-30} Cm	67.5 ± 0.6	59.7 ± 3.3	73.0 ± 0.8	58.3 ± 0.5
c^2		0.10 ± 0.00	0.11 ± 0.01	0.16 ± 0.01	0.26 ± 0.01

A similar EOA characterization for compounds **5a** and **6a** was previously reported by us.[9]

The addition of the second nitro substituent in **2** and **4** could be responsible for the appearance of a second CT transition polarized perpendicularly to μ_g, as already observed for 3,5-dinitroaniline.[7,21] The CT band of **4** in 1,4-dioxane shows asymmetry in the higher energy slope, which could arise from overlapping of two transitions. The multilinear fitting of the EOA spectra of **4** (Figure 1B) was then limited to the longer wavelength region of the CT band, to avoid mixing of the two molecular excited states. For **2** a similar analysis is precluded, as the local transitions and the CT band are close in energy.

The EOA spectrum is regulated by two effects: the electrodichroic and Stark effects. The former is caused by reorientation of the chromophores in the externally applied electric field and can be measured through the regression coefficient E. A positive ($E>0$) electrodichroism is observed when the absorption increases for parallel polarization ($\varphi=0°$) and decreases for orthogonal polarization ($\varphi=90°$). This happens when μ_g and μ_{eg} are essentially parallel. The second effect is the band shift of the CT band in the presence of the electric field. It only occurs when the optical excitation is accompanied by a change in dipole moment. A bathochromic shift relative to the absorption spectrum shows an increase in the molecular dipole moment on going from ground to excited state ($\Delta\mu>0$).

All of the chromophores show positive electrodichroism. The monodimensional approximation is valid and the TLM can be safely applied. With the only exception of **5a** ($0.0<\varepsilon_{rL}<2.2$),[9] a bathochromic shift of the EOA spectra with respect to the conventional UV/Vis spectra is observed in 1,4-dioxane. This result is consistent with a predominant **NE** character of their ground states. Considering values from Table 3 and c^2 values of **5a** and **6a** (0.56 and 0.46, respectively),[9] an extended range of ground-state electronic distribution ($0.11<c^2<0.56$) is observed for **1–6** in 1,4-dioxane as a consequence of the variety in bridging units, donor groups, and annelation. The ground-state polarization is more affected by the change in the bridging unit (**1** vs. **3** and **2** vs. **4**) than by the addition of the second nitro group. The important effect of the nature of the bridge is transferred to the derived β_0 values. The first hyperpolarizability increases approximately by a factor of three on going from **1** to **3** and by a factor of two from **2** to **4**. Compound **3** has the largest value in 1,4-dioxane. Compounds **5a** and **6a**, the c^2 values of which are closer to the cyanine limit than those of chromophores **1–4**, show the highest $\delta\alpha_0$ values. This result is a consequence of the strong increase in ground-state dipole moment on going from **1–4** to **5a** and **6a** (Tables 2 and 3); this effect is directly correlated to the increase in **ZW** character, that is, a c^2 value closer to 1. In contrast, both the addition of a second nitro group (from **1** to **2** and from **3** to **4**) and the change of the bridging unit from methino (**3** and **4**) to azomethino (**1** and **2**), which had a significant role in affecting the ground-state polarization (c^2), have a negligible effect on μ_g (within the experimental error, ±5%). Quite unexpected is the fact that the estimated $\Delta\mu_{max}$ values for dinitrophenyl derivatives **2** and **4** are lower than those of their mononitro counterparts.

Quantum-chemical modeling

Need for a computational approach: Owing to the strong electric field required for EOA measurements, spectra are recordable only in solvents with low dielectric constants to avoid dielectric breakdown. This limit prevents the study of β_0 and μ_g in solvents covering a wide range of polarity. Thus, a detailed experimental investigation of the effect of solvent polarity on the PR molecular parameters is precluded.

We have previously investigated the dependence of the first hyperpolarizability β_0 on the surrounding polarity through ab initio quantum mechanical computations on compounds **5a** and **6a** at the restricted Hartree–Fock (RHF) level of theory with 6-31G* basis set and inclusion of the solvent effect by using Onsager's self-consistent reaction-field (SCRF) model.[9] Since the applied computational framework proved to be a powerful tool for investigating the effect of medium polarity on the molecular nonlinear optical (NLO) properties of push–pull molecules, we followed a similar approach with the aim of extending the investigation of μ_g and β_0 to solvents in which the experimental data are not available.

Computational details: Structural and electronic properties of dyes **1–6** were investigated by computations. Derivatives **5b** and **6b** were taken as models for molecules **5a** and **6a**, respectively.[9] All ab initio computations used the Gaussian 98[22] program package.[23] Full geometry optimizations and frequency analyses were performed at the RHF and DFT[24] levels of theory with 6-31G* basis set.[25] Compounds **5b** and **6b** were computed within C_s symmetry constraints; C_s and C_1 symmetries were considered for dyes **1–4**. Solvent effects on structures, electronic parameters, $\delta\alpha_0$, and β_0 were included by using Onsager's SCRF approach,[26] as available in the Gaussian package. Since a spherical cavity is not the best approximation for elongated chromophores, we also checked the effect of the Tomasi polarized continuum model (PCM)[27] and of the self-consistent isodensity polarized continuum model (SCI-PCM,[28] as implemented in the Gaussian 98 package) on the prediction of the ground-state dipole moment of **3** and **5b**. Data for **3** show that Onsager's SCRF model leads to a slight overestimation of μ_g at high ε_r values in comparison to the other models (Supporting Information). For derivative **5b** the implementation of PCM and SCI-PCM solvent cavities did not satisfy convergence criteria during geometry optimization. Owing to the significant computational cost of including different solvent models and the opportunity to have a set of consistent data for all of the compounds, we chose to limit the investigation of the SCRF solvent effect to the Onsager model.[29] The use of the SCRF approach to model with accuracy and efficiency the effects of solvent polarity on structure and NLO molecular properties has been recently reported.[9,30] Huyskens et al.

investigated the effect of specific solute–solvent interactions on the NLO properties of *N*,*N*-dimethyl-*p*-nitroaniline and found that the formation of hydrogen bonds in solvents such as $CHCl_3$ or CH_2Cl_2 (but not DMSO) increases the first hyperpolarizability β.[31] We believe that similar hydrogen-bonding interactions between $CHCl_3$, which is among the solvents considered in the present work, and the imine nitrogen atom of compounds **1** and **2** are unlikely on the basis of our previous ^{15}N NMR investigation.[14] Indeed, the ^{15}N chemical shift of the imine nitrogen atom of **1** in $CHCl_3$ is even slightly shifted to high field (234 ppm relative to liquid NH_3) with respect to the corresponding value in DMSO (236 ppm). On the basis of this, explicit effects from solvent molecules have been neglected.

Ground-state energies and geometries: Absolute energies and frequency analysis [number of imaginary frequencies (NIMAG)] of the computed structures for selected solvent–cavity polarities are summarized in the Supporting Information. Computed C_1 geometries of **1**–**4** were characterized as minima (zero imaginary frequencies) in each solvent. In contrast, up to three imaginary frequencies were calculated for C_s optimized structures. An analysis of these imaginary frequencies revealed that the lowest ones were associated with rotation of the *N*-methyl or 2-nitro group, whereas the highest one was due to a significant deviation from planarity. Only one imaginary frequency, corresponding to rotation of the *N*-methyl group, was computed at the B3LYP level for **5b** and **6b** (up to three imaginary frequencies were found for RHF/6-31G* computed C_s structures).[9] On this basis, we conclude that the C_s optimized structures of **5b** and **6b** are true minima. We therefore used optimized C_1 structures of **1**–**4** and C_s structures of **5b** and **6b** in the subsequent analysis of data and discussion.

The RHF/6-31G* optimized structures of **1**, **3**, and **5b** in the gas phase and DMSO are shown in Figure 2. The effects of the addition of a second nitro group in **2** and **4** and benzo fusion of the azine ring in **6b** are of secondary importance with respect to the effect of varying the bridging unit or the donor moiety. Selected geometrical parameters (dihedral angles between the two aromatic rings in **1**–**4** and azine–bridge bond lengths in **1**–**4**, **5b**, and **6b**) are listed in the Supporting Information. The most evident feature in C_1 optimized structures of **1** and **3** is a significant deviation from planarity. As expected, such deviation increases in **2** and **4** due to the addition of a second nitro group in the position *ortho* to the bridge. As solvent polarity increases, geometries tend to flatten and the azine–bridge bond elongates, as a consequence of increased **ZW** character. Such bond elongation is particularly evident for compounds **5b** and **6b** (DFT computed bond lengths increase from 1.39 Å in the gas phase to 1.46–1.47 Å in DMSO).

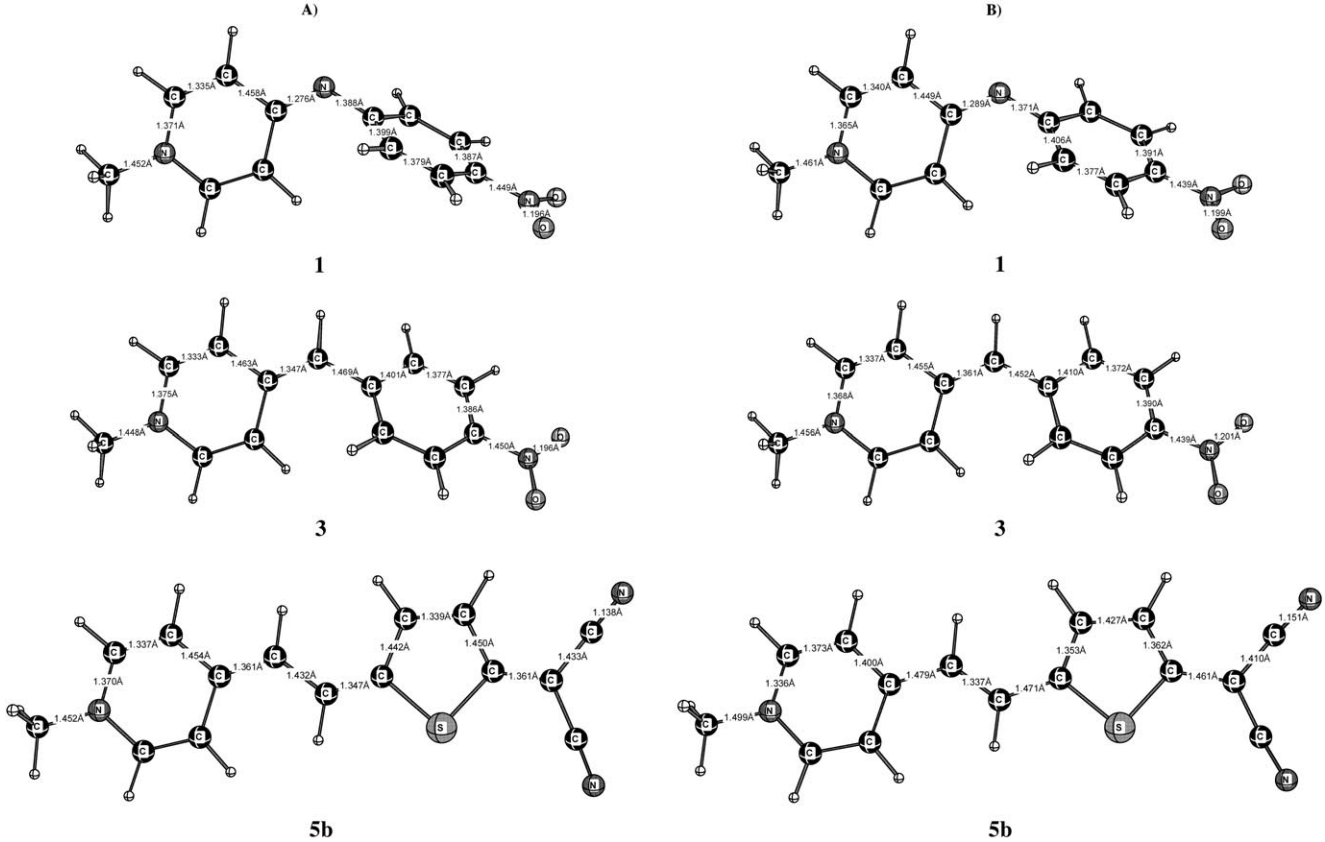

Figure 2. Optimized ground-state geometries (RHF/6-31G*) in the gas phase (A) and DMSO (B). Structures of **5b** are taken from reference [9].

Dipole moment, polarizability anisotropy, and hyperpolarizability: Table 2 lists computed RHF/6-31G* and B3LYP/6-31G* ground-state dipole moments, polarizability anisotropy, and first hyperpolarizability for **1**–**4** (C_1 symmetry) and **5b** and **6b** (C_S symmetry). Ground-state dipole moments and static polarizability anisotropies were obtained from the computed tensor components according to Equations (9) and (3), respectively. Computed static first hyperpolarizabilities were obtained by the coupled perturbed Hartree–Fock (CPHF)[32] method. Starting from the computed values of the static ten independent components [β_{ijk} ($i, j, k = x, y, z$)] and adopting Kleinman symmetry relations, we calculated $\beta_{0,vec}$ (the component along the dipole axis) and $\beta_{0,tot}$ according to Equations (10)–(12).[33,34] Calculated β_0 values were corrected according to the Taylor convention used in the EOA measurements to be consistent with the experimental data.[35] The predicted $\beta_{0,vec}$ values for derivatives **5b** and **6b** have been previously reported[9] and were used in the present work in order to predict the trend of the static figures of merit (F_0^L and F_0^H). Plots of RHF/6-31G*[36] computed parameters of selected compounds **1**, **3**, and **5b** as a function of solvent-cavity polarity are shown in Figure 3.

$$\mu_g = \sqrt{\mu_x^2 + \mu_y^2 + \mu_z^2} \tag{9}$$

$$\beta_i = \beta_{iii} + \frac{1}{3}\sum_{i \neq k} (\beta_{ikk} + \beta_{kik} + \beta_{kki}) \quad i,k = x,y,z \tag{10}$$

$$\beta_{0,vec} = \frac{\mu_x\beta_x + \mu_y\beta_y + \mu_z\beta_z}{|\mu_g|} \tag{11}$$

$$\beta_{0,tot} = \sqrt{\beta_x^2 + \beta_y^2 + \beta_z^2} \tag{12}$$

As expected, the ground-state dipole moment increases monotonically as a function of solvent-cavity polarity and levels off at large values of ε_r. The increase in μ_g is in agreement with a more important contribution of the **ZW** limiting form. The trend observed for the polarizability anisotropy and hyperpolarizability is different if one considers dyes **1** and **3** or dye **5b**. A monotonic behavior of $\delta\alpha_0$ and $\beta_{0,vec}$ against ε_r is observed for the first two dyes. The largest value is reached at the right end of the graph, corresponding to high surrounding polarity. In contrast, the predicted trend of $\delta\alpha_0$ and β_0 for **5b** is not monotonic, as a consequence of the fact that in some polarity regions the **NE** form predominates, whereas in others the **ZW** character is more important.[9] In general, computed $\beta_{0,vec}$ and $\beta_{0,tot}$ values are similar. A difference between the two values is computed for dyes **2** and **4** (e.g., 5×10^{-50} vs. 8×10^{-50} C V^{-2} m^3 and 32×10^{-50} vs. 37×10^{-50} C V^{-2} m^3 in 1,4-dioxane for **2** and **4**, respectively) as a consequence of deviation from the monodimensional approximation, likely due to the presence of a second nitro substituent. However, the computed trends of $\beta_{0,vec}$ and $\beta_{0,tot}$ being very similar, only $\beta_{0,vec}$ values (from now on simply called β_0) were considered in the following discussion of NLO properties. Solvent-dependent computed

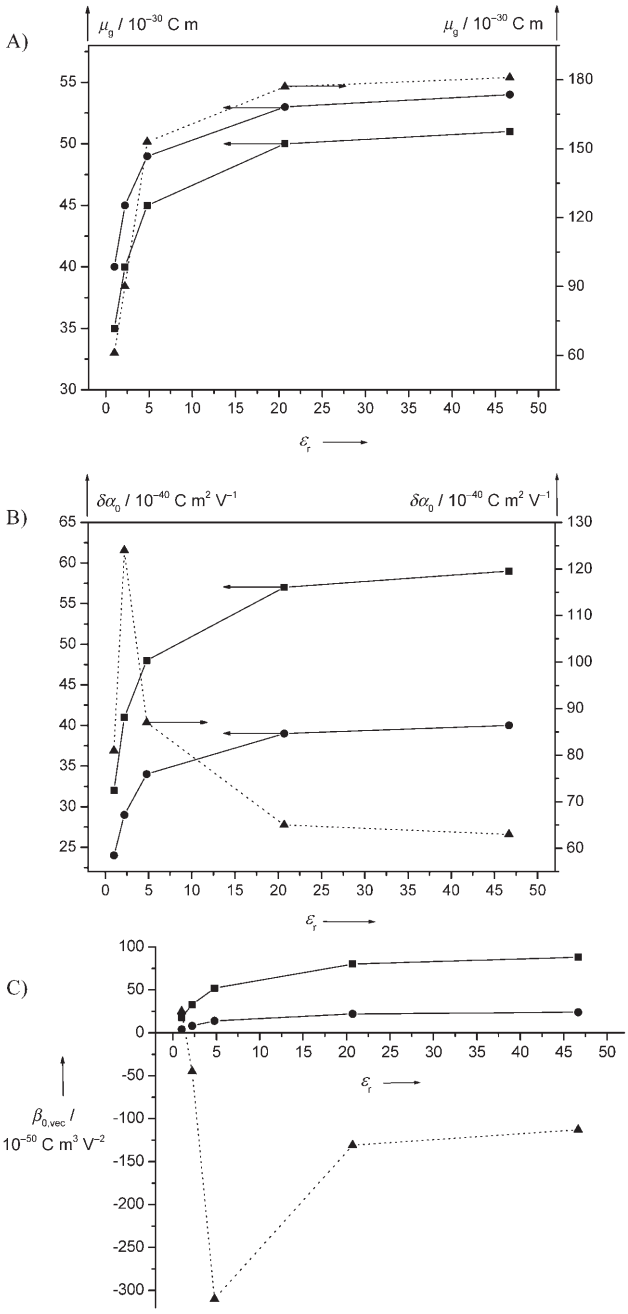

Figure 3. RHF/6-31G* computed ground-state dipole moment μ_g (A), polarizability anisotropy $\delta\alpha_0$ (B), and first hyperpolarizability $\beta_{0,vec}$ (C) of compounds **1** (●, C_1 symmetry), **3** (■, C_1 symmetry), and **5b** (▲, C_s symmetry). The lines are guides for the eyes. Arrows indicate the *y* axis corresponding to the plot.

angles between the vector $\boldsymbol{\mu}_g$ and the tensor $\boldsymbol{\beta}$, reduced to a first-rank tensor, are listed in the Supporting Information.

Structural and solvent-polarity control of ground-state parameters: The combination of different experimental and computational studies gained important insights into the effect of chemical units (donors, acceptors, and spacers) and solvent polarity on relevant ground-state and NLO parameters. In particular, it was possible to correlate the trend of

Table 4. Experimental[a] and computed[b] figures of merit of high- (F_0^H) and low-T_g (F_0^L) PR materials for compounds **1–6** in selected media.[c]

(ε_r)		Gas phase (1.0)		1,4-Dioxane (2.2)		$CHCl_3$ (4.8)		Acetone (20.7)		DMSO (46.7)	
		F_0^L	F_0^H	F_0^L	F_0^H	F_0^L	F_0^H	F_0^L	F_0^H	F_0^L	F_0^H
1	exptl			0.35	0.70						
	comp	0.82	0.07	1.27	0.16	1.76	0.29	2.40	0.50	2.56	0.56
2	exptl			0.25	0.45						
	comp	0.59	0.03	1.09	0.08	1.72	0.18	2.54	0.34	2.76	0.38
3	exptl			0.74	1.74						
	comp	0.87	0.27	1.46	0.58	2.14	1.02	3.16	1.75	3.43	1.96
4	exptl			0.60	0.90						
	comp	0.84	0.27	1.50	0.55	2.42	0.93	4.01	1.41	4.52	1.49
5	exptl[d]			5.24	−1.57						
	comp[e,f]	3.84	0.39	12.50	−1.03	24.15	−12.11	24.78	−5.94	25.22	−5.23
6	exptl[d]			3.67	0.84						
	comp[e,f]	2.86	0.42	9.47	0.85	24.79	−12.18	26.27	−5.05	27.03	−4.22

[a] From optical and electro-optical absorption measurements. [b] From RHF/6-31G*//RHF/6-31G* ab initio calculations; **1–4**: C_1 symmetry; **5b** and **6b**: C_s symmetry. [c] $F_0^H/10^{-76}\,C^2V^{-2}\,m^4kg^{-1}mol$; $F_0^L/10^{-74}\,C^2V^{-2}\,m^4kg^{-1}mol$); data were calculated according to the Taylor convention.[9]. [d] Derivatives **a**. [e] Derivatives **b**. [f] To be directly comparable with experimental data, evaluations of figures of merit from computations on derivatives **b** took into account the same alkyl chains as in derivatives **a**.

the variation of μ_g, $\delta\alpha_0$, and β_0 to the chemical nature of the building blocks and to the polarity of the surrounding medium, which in turn determined the contribution of the **NE** and **ZW** limit formulas to the description of the chromophore's ground state. In general, computed μ_g and $\delta\alpha_0$ values were somewhat larger and β_0 smaller than experimental data. We determined that the Onsager model leads to an overestimation of the computed μ_g values (Supporting Information). It is likely that the discrepancy found for $\delta\alpha_0$ and β_0 is partially caused by the used solvation model and the implemented levels of theory. However, the computed trends found for μ_g, $\delta\alpha_0$, and β_0 as a function of structural modification and surrounding polarity agree well with the experimental evidence. On this basis, the predicted values of β_0 and μ_g in media where experimental data are not accessible may be considered highly reliable. Experimental polarizability anisotropies were available in different solvents, and a good agreement with computational data has been found. The increase of $\delta\alpha_0$ in dyes **1–4** at larger polarities is in agreement with a predominant **NE** character. Their geometrical and electronic structure varies along a path going from the polyene to the cyanine limit. In contrast, dyes **5** and **6** show a decrease of their $\delta\alpha_0$ in polar surroundings, due to a predominant **ZW** character. Their geometric and electronic structure varies along a path going from a cyanine-like structure to the zwitterionic limit.

The different behaviors found against ε_r find confirmation in the CT band-shape analysis. As the polarity of the medium is increased the CT band becomes sharper for dyes **1–4** and broader for **5** and **6**. Overlapping UV/Vis spectra of **2** in different media are shown in the Supporting Information. This result is in full agreement with the previous conclusions, that is, dyes **1–4** move towards the cyanine limit as polarity increases, whereas **5** and **6** move away from it. Close to the cyanine limit a "charge-resonant" character of the electronic transition becomes important, and the difference between ground- and excited-state geometries tends to a minimum, which results in sharpening of the band.[5a,7,37]

Photorefractive molecular sensitivity: structural and solvent effects: F_0^L and F_0^H values, calculated from experimental and computed data by applying Equations (1) and (2), are collected in Table 4. Plots of the computed static low- and high-T_g figures of merit as a function of solvent polarity for representative compounds **1**, **3**, and **5** are shown in Figure 4.

The F_0^L value increases as a function of the surrounding polarity for all of the dyes. Such a growth is monotonic for **1** and **3**, and F_0^L levels off only in very polar solvents. Somewhat different is the behavior of **5**, for which a plateau is reached also in weakly polar media and the strongest variation is computed for a small range of ε_r corresponding to the switch from **NE** to **ZW** character. The variation of low-T_g PR performance of **5** covers approximately one order of magnitude.

The dependence of F_0^H on medium polarity strongly reflects that found for β_0 as a direct consequence of the definition of this parameter [Eq. (2)]. Accordingly, a monotonic increase is observed for **1** and **3**, with a plateau at high polarities similar to what is found for F_0^L. The predicted enhancement of the high-T_g performance of **3** is close to one order of magnitude. The F_0^H value of **5** peaks at intermediate polarities, with an enhancement with respect to smallest values by nearly two orders of magnitude. The PR performance levels off at the two polarity extremes. Therefore a very restricted range of medium polarity corresponds to optimized performance for this type of systems.

Conclusion

Complementary experimental and computational tools have been used to gain new insights into the PR molecular properties of push–pull dipolar chromophores in terms of structural and medium-polarity effects. This method has been applied to two classes of heteroaromatic-based dyes, rather different in structural and electronic properties. Dyes **1–4** are predominantly **NE**, whereas compounds **5** and **6** are pre-

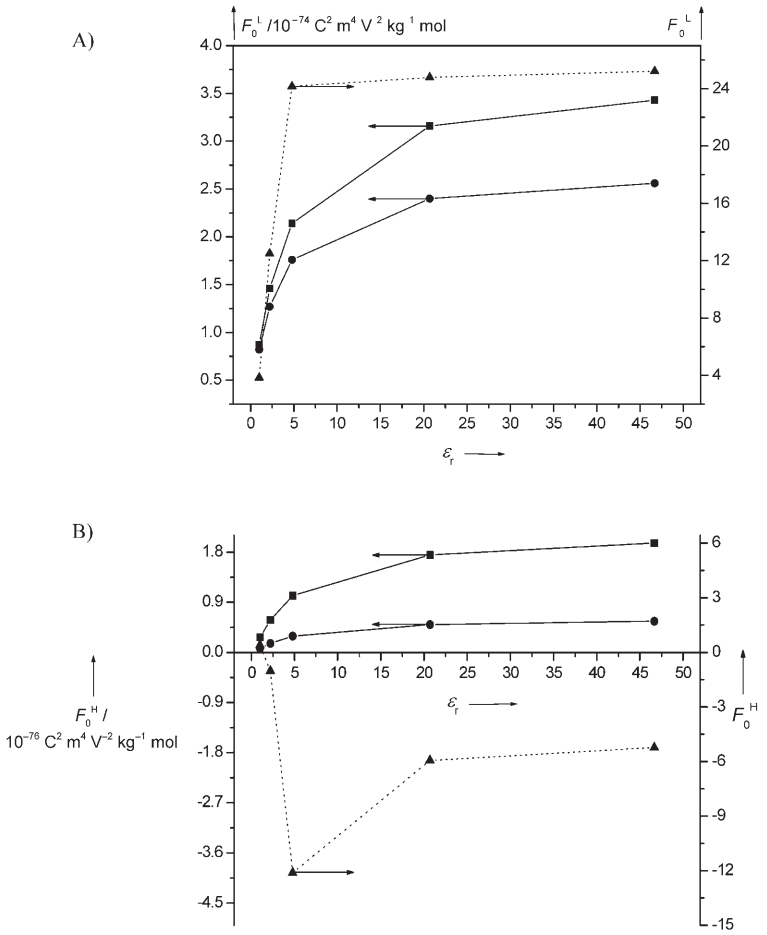

Figure 4. RHF/6-31G* computed static figure of merit for low-T_g (A) and high-T_g (B) PR materials of compounds **1** (●, C_1 symmetry), **3** (■, C_1 symmetry), and **5** (▲, C_s symmetry). The lines are guides for the eyes. Arrows indicate the *y* axis corresponding to the plot.

dominantly **ZW**, with the **NE**/**ZW** relative contribution varying as a function of solvent polarity. A precise combination of donor, acceptor, and spacer groups was carefully selected to give rise to a number of molecules with variable structural and electronic features. Together with the figures of merit for low- and high-T_g PR materials, all the relevant ground-state and NLO molecular parameters have been experimentally determined and computationally investigated. The computational study at the RHF and DFT levels of theory was able to circumvent the limits of the spectroscopic measurements dictated by the restricted choice of a solvent compatible with the strong external electric field. Predicted trends were always in good agreement with the experimental data and thus provided a rather thorough picture of the PR molecular sensitivity in terms of structural and solvent-polarity effects.

This study has established for the first time the strategic role of the polarity of the surrounding medium in determining PR molecular performance. The effect of the polarity, in combination with structural effects, is so remarkable that the induced change in low- and high-T_g PR response spans around one or two orders of magnitude, depending on the molecular system. The intrinsic PR activity of a given compound may be spoiled by an unfortunate or arbitrary choice of medium (solvent or solid matrix). On the other hand careful selection of the host matrix may lead to optimized performances, with enhancements by orders of magnitude, and this suggests that careful tuning of the medium polarity can be used as a new powerful tool for maximizing the molecular PR response. In particular, the large sensitivity of a system such as **5** in the $2.5 < \varepsilon_r < 10$ range (Figure 4) can be translated to the bulk by choosing host matrices such as polymaleimide ($\varepsilon_r = 3.1$–3.3), poly(methyl methacrylate) ($\varepsilon_r = 3.2$–3.5), poly(ethylene glycol) ($\varepsilon_r = 3.6$–4.0), or sol–gel glasses ($\varepsilon_r > 6$), the polarity of which should be optimal according to the predicted trend of the PR figure of merit for high-T_g materials. It is quite intriguing that a combination of molecular design and host-matrix engineering can be systematically used for generation of new high-performance PR materials.

Experimental Section

Materials: Compounds **1**–**4**,[14] **5a**,[16] and **6a**[9] were prepared and purified according to literature protocols.

UV/Vis absorption measurements: UV/Vis spectra were recorded with a UV/Vis/NIR Jasco V 570 spectrophotometer at room temperature (298 K). Quartz cuvettes of different thickness (1 and 10 cm) were used. Data were collected every 0.5 nm with a recording speed of 400 nm min^{-1}. All of the solvents used for conventional UV/Vis measurements were carefully dried and purified according to literature procedures.[38]

Electro-optical absorption measurements: The EOA characterization was carried out following previously described methods.[7,19] *p*-Amino-*p*′-nitrobiphenyl was used as a calibrating reference. All measurements were performed at 298 K, recording the EOA signal every 10 nm with an integration time of 0.8–1 min (depending on the quality of the signal). All EOA spectra were recorded in anhydrous 1,4-dioxane, prepared by distillation from Na/K alloy under argon prior to use. Supplementary optical absorption spectra required for the evaluation of the EOA spectra were recorded in 1,4-dioxane with a Perkin-Elmer Lambda 900 spectrophotometer at 298 K (scan speed of 100 nm min^{-1}, 3 cm quartz glass cuvette).

Acknowledgements

This work was partially supported by MIUR-FIRB (Grant RBNE01P4JF), MIUR-PRIN (Grant 2001034442), and Deutsche Forschungsgemeinschaft. We thank Prof. Dr. H.-G. Kuball and Prof. Dr. G. A. Pagani for helpful discussions and valuable suggestions.

[1] O. Ostroverkhova, W. E. Moerner, *Chem. Rev.* **2004**, *104*, 3267–3314.
[2] S. Ducharme, J. C. Scott, R. J. Twieg, W. E. Moerner, *Phys. Rev. Lett.* **1991**, *66*, 1846–1849.
[3] J. S. Schildkraut, *Appl. Phys. Lett.* **1991**, *58*, 340–342.
[4] P. Günter, J. P. Huignard, *Photorefractive Effects and Materials, Vol. 61–62*, Springler, New York, **1988**.
[5] a) R. Wortmann, C. Poga, R. J. Twieg, C. Geletneky, C. R. Moylan, P. M. Lundquist, R. G. DeVoe, P. M. Cotts, H. Horn, J. E. Rice, D. M. Burland, *J. Chem. Phys.* **1996**, *105*, 10637–10647; b) R. Wortmann, C. Glania, P. Krämer, K. Lukaszuk, R. Matschiner, R. J. Twieg, F. You, *Chem. Phys.* **1999**, *245*, 107–120.
[6] W. E. Moerner, S. M. Silence, F. Hache, G. C. Bjorklund, *J. Opt. Soc. Am. B* **1994**, *11*, 320–330.
[7] J. J. Wolff, R. Wortmann, *Adv. Phys. Org. Chem.* **1999**, *32*, 121–217.
[8] a) S. R. Marder, B. Kippelen, A. K.-Y. Jen, N. Peyghambarian, *Nature* **1997**, *388*, 845–851; b) C. Dehu, F. Meyers, E. Hendrickx, K. Clays, A. Persoons, S. R. Marder, J. L. Brédas, *J. Am. Chem. Soc.* **1995**, *117*, 10127–10128.
[9] A. Abbotto, L. Beverina, S. Bradamante, A. Facchetti, C. Klein, G. A. Pagani, M. Redi-Abshiro, R. Wortmann, *Chem. Eur. J.* **2003**, *9*, 1991–2007.
[10] a) S. R. Marder, J. W. Perry, G. Bourhill, C. B. Gorman, B. G. Tiemann, K. Mansour, *Science* **1993**, *261*, 186–189; b) M. Barzoukas, C. Runser, A. Fort, M. Blanchard-Desce, *Chem. Phys. Lett.* **1996**, *257*, 531–537; c) W. H. Thompson, M. Blanchard-Desce, V. Alain, J. Muller, A. Fort, M. Barzoukas, J. T. Hynes, *J. Phys. Chem.* **1999**, *103*, 3766–3771.
[11] J. L. Oudar, D. S. Chemla, *J. Chem. Phys.* **1977**, *66*, 2664–2668.
[12] M. Barzoukas, M. Blanchard-Desce, *J. Chem. Phys.* **2000**, *112*, 2036–2044.
[13] F. Wünther, R. Wortmann, K. Meerholz, *ChemPhysChem* **2002**, *3*, 17–31.
[14] A. Abbotto, S. Bradamante, G. A. Pagani, *J. Org. Chem.* **2001**, *66*, 8883–8892.
[15] a) A. Abbotto, S. Bradamante, A. Facchetti, G. A. Pagani, I. Ledoux, J. Zyss, *Mater. Res. Soc. Symp. Proc.* **1998**, *488*, 819–822; b) A. Abbotto, S. Bradamante, A. Facchetti, G. A. Pagani, L. Yuan, P. N. Prasad, *Gazz. Chim. Ital.* **1997**, *127*, 165–166.
[16] A. Abbotto, S. Bradamante, A. Facchetti, G. A. Pagani, *J. Org. Chem.* **1997**, *62*, 5755–5765.
[17] According to the two-level model, the sign of $\beta(-\omega;\omega,0)$ changes from positive to negative when the character of the ground-state electronic distribution changes from **NE** ($c^2<0.5$) to **ZW** ($c^2>0.5$).
[18] a) W. Liptay, in *Excited States, Vol. 1, Dipole Moments and Polarizabilities of Molecules in Excited Electronic States* (Ed.: E. C. Lim), Academic Press, New York, **1974**, pp. 129–229; b) R. Wortmann, K. Elich, S. Lebus, W. Liptay, P. Borowicz, A. Grabowska, *J. Phys. Chem.* **1992**, *96*, 9724–9730.
[19] a) S. Beckmann, K.-H. Etzbach, P. Krämer, K. Lukaszuk, R. Matschiner, A. J. Schmidt, P. Schumacher, R. Sens, G. Seibold, R. Wortmann, F. Würthner, *Adv. Mater.* **1999**, *11*, 536–541; b) F. Würthner, C. Thalacker, R. Matschiner, K. Lukaszuk, R. Wortmann, *Chem. Commun.* **1998**, *16*, 1739–1740.
[20] F. Steybe, F. Effenberger, P. Krämer, C. Glania, R. Wortmann, *Chem. Phys.* **1997**, *219*, 317–331.
[21] R. Wortmann, P. Krämer, C. Glania, S. Lebus, N. Detzer, *Chem. Phys.* **1993**, *173*, 99–108.
[22] Gaussian 98, Revision A.11.3, M. J. Frisch, G. W. Trucks, H. B. Schlegel, G. E. Scuseria, M. A. Robb, J. R. Cheeseman, V. G. Zakrzewski, J. A. Montgomery, Jr., R. E. Stratmann, J. C. Burant, S. Dapprich, J. M. Millam, A. D. Daniels, K. N. Kudin, M. C. Strain, O. Farkas, J. Tomasi, V. Barone, M. Cossi, R. Cammi, B. Mennucci, C. Pomelli, C. Adamo, S. Clifford, J. Ochterski, G. A. Petersson, P. Y. Ayala, Q. Cui, K. Morokuma, N. Rega, P. Salvador, J. J. Dannenberg, D. K. Malick, A. D. Rabuck, K. Raghavachari, J. B. Foresman, J. Cioslowski, J. V. Ortiz, A. G. Baboul, B. B. Stefanov, G. Liu, A. Liashenko, P. Piskorz, I. Komaromi, R. Gomperts, R. L. Martin, D. J. Fox, T. Keith, M. A. Al-Laham, C. Y. Peng, A. Nanayakkara, M. Challacombe, P. M. W. Gill, B. Johnson, W. Chen, M. W. Wong, J. L. Andres, C. Gonzalez, M. Head-Gordon, E. S. Replogle, and J. A. Pople, Gaussian, Inc., Pittsburgh PA, **2002**.
[23] Computations were carried out at the Cineca Supercomputer Center in Bologna (Italy) on SGI Origin 3800 and IBM SP RS/6000 Power3 machines.
[24] DFT calculations used the B3LYP functional: a) A. D. Becke, *J. Chem. Phys.* **1993**, *98*, 5648–5652; b) V. Barone, *J. Chem. Phys.* **1994**, *101*, 6834–6838.
[25] The effect of larger basis sets, such as 6-31G** and 6-311G**, was tested in computing the ground-state properties of compound **3**. Since no significant differences were recorded with respect to 6-31G* calculations, they were not used any longer in this work.
[26] a) L. Onsager, *J. Am. Chem. Soc.* **1936**, *58*, 1486–1493; b) M. W. Wong, M. J. Frisch, K. B. Wiberg, *J. Am. Chem. Soc.* **1991**, *113*, 4776–4782.
[27] S. Miertus, J. Tomasi, *Chem. Phys.* **1982**, *65*, 239–245.
[28] J. B. Foresman, T. A. Keith, K. B. Wiberg, J. Snoonian, M. J. Frisch, *J. Phys. Chem.* **1996**, *100*, 16098–16104.
[29] Gas-phase optimized structures were used as starting geometries in SCRF calculations. The radius of the Onsager spherical cavity was set 20% larger than the value predicted by gas-phase calculations in order to account for the nonspherical geometries of the dyes. For a given compound this value was kept constant in each solvent.
[30] a) P. C. Ray, *Chem. Phys. Lett.* **2004**, *395*, 269–273; b) R. Cammi, R., B. Mennucci, J. Tomasi, *J. Phys. Chem. A* **2000**, *104*, 4690–4698; c) Y. Luo, P. Norman, P. Macak, H. Agren, *J. Chem. Phys.* **1999**, *111*, 9853–9858.
[31] F. L. Huyskens, P. L. Huyskens, A. P. Persoons, *J. Chem. Phys.* **1998**, *108*, 8161–8171.
[32] a) J. Gerratt, I. M. Mills, *J. Chem. Phys.* **1968**, *49*, 1730–1739; b) G. J. B. Hurst, M. Dupuis, E. Clementi, *J. Chem. Phys.* **1988**, *89*, 385–395; c) H. Sekino, R. J. Bartlett, *J. Chem. Phys.* **1991**, *94*, 3665–3669; d) S. P. Karna, M. Dupuis, *J. Comput. Chem.* **1991**, *12*, 487–504.
[33] a) D. M. Bishop, *Rev. Mod. Phys.* **1990**, *62*, 343–374; b) D. R. Kanis, M. A. Ratner, T. J. Marks, *Chem. Rev.* **1994**, *94*, 195–242; c) J. L. Oudar, *J. Chem. Phys.* **1977**, *67*, 446–457; d) D. M. Bishop, *Molecular Vibrations and Nonlinear Optics in Advances in Chemical Physics* (Eds.: I. Prigogine, S. A. Rice), Wiley, New York, **1998**; e) J. J. P. Stewart, *J. Comput. Chem.* **1989**, *10*, 221–264.
[34] a) D. A. Kleinman, *Phys. Rev.* **1962**, *126*, 1977–1979; b) C. Bosshard, K. Sutter, P. Prêtre, J. Hulliger, M. Flörsheimer, P. Kaatz, P. Günter, *Organic Nonlinear Optical Materials—Advances in Nonlinear Optics, Vol. 1* (Eds.: A. F. Garito, F. Kajzar), Gordon and Breach, Basel, **1995**.
[35] A. Willets, J. E. Rice, D. M. Burland, D. P. Shelton, *J. Chem. Phys.* **1992**, *97*, 7590–7599.
[36] The B3LYP/6-31G* predicted trends for μ_g and $\delta\alpha_0$ are similar to those computed at the RHF/6-31G* level of theory.
[37] F. Würthner, R. Wortmann, R. Matschiner, K. Lukaszuk, K. Meerholz, Y. DeNardin, R. Bittner, C. Bräuchle, R. Sens, *Angew. Chem.* **1997**, *109*, 2933–2936; *Angew. Chem. Int. Ed. Engl.* **1997**, *36*, 2765–2768.
[38] W. L. F. Armarego, D. D. Perrin, *Purification of Laboratory Chemicals*, 4th ed., Butterworth-Heinmann, **1996**.

Received: January 9, 2006
Revised: April 29, 2006
Published online: July 5, 2006

